arXiv:1207.3995v1 [cond-mat.mtrl-sci] 17 Jul 2012

Prediction of bias voltage dependent magnetic contrast from spin-polarized tunneling spectroscopy

Krisztián Palotás*
Budapest University of Technology and Economics,
Department of Theoretical Physics, Budafoki út 8., H-1111 Budapest, Hungary

(Dated: July 18, 2012)

We propose a method to estimate the bias voltage dependent magnetic contrast observed on constant current spin-polarized scanning tunneling microscopy (SP-STM) images from single point differential conductance (dI/dV) tunneling spectra. Depending on the number of single point measurements, the bias positions of magnetic contrast reversals and the maximally achievable magnetic contrast can be determined. We validate this proposal by simulating SP-STM images on a complex magnetic surface by employing a recently developed approach based on atomic superposition. Furthermore, we show evidence that the tip electronic structure has a major effect on the magnetic contrast. Our theoretical prediction should inspire experimentalists to considerably reduce measurement efforts for determining the bias dependent magnetic contrast on magnetic surfaces.

PACS numbers: 72.25.Ba, 68.37.Ef, 71.15.-m, 73.22.-f

Achieving ultrahigh information density in a controlled way on surfaces of materials [1, 2] is one of the ultimate goals of magnetic research nowadays for the purpose of future data storage technological applications. This can be established by the reduction of the size of magnetic information storage units going down to the nanoscale or even to single atoms [3]. Reading and writing information routinely from and to such magnetic units is a great challenge. Spin-polarized scanning tunneling microscopy (SP-STM) [4], employing a magnetic tip, proved to be extremely successful for studying magnetism on surfaces in high spatial resolution. Recent experimental advances using this technique allow the investigation of complex magnetic structures (frustrated antiferromagnets, spin spirals, skyrmion lattices, etc.) [3, 5–7].

In the most routinely used constant current mode of SP-STM, the apparent height difference between differently magnetized surface atoms allows the discrimination of the individual atomic magnetic properties and the mapping of the magnetic structure. This apparent height difference is called magnetic contrast. Finding the maximal magnetic contrast for a given surface-tip combination is crucial for a more efficient magnetic mapping. This can be done by using magnetic tips with large spin polarization, or, by choosing the appropriate bias voltage. A very few works focused on the investigation of the bias dependent magnetic contrast so far. Among those, a magnetic contrast reversal has been reported in two different magnetic systems [8, 9], and the effect was related to the surface electronic structure rather than to the effect of the tip. In another work, such contrast reversals were observed during the scanning with the STM tip at fixed bias, and this was identified to be due to the magnetic switching of the tip [10]. Moreover, under certain circumstances, a giant magnetic contrast can be obtained, and this effect was explained by chemically modified STM tips [11].

Distinguishing atoms with different magnetic properties on a complex magnetic surface can successfully be performed by spin-polarized scanning tunneling spectroscopy (SP-STS) as well. For example this technique has recently been used to read out information from an atomic scale all-spin-based logic device [12]. Here, through scanning the surface with a magnetic tip, the measured differential conductance (dI/dV) values vary depending on the magnetic properties of the underlying surface atom. For such a spectroscopic detection of atomic magnetism, the contrast, that is the dI/dV difference above individual atoms, should also be tunable by changing the bias voltage [13].

In this work, we propose a method to estimate the bias dependent magnetic contrast observed in constant current SP-STM experiments from single point differential conductance tunneling spectra. The key quantity for this estimation is the magnetic contribution to the differential conductance, dI_{MAGN}/dV, that can be obtained from measuring tunneling spectra with oppositely magnetized tips. Let us assume that one can measure differential conductances $dI_P^A/dV(z_1,V)$ and $dI_{AP}^A/dV(z_1,V)$ at the same tip position above surface atom A at z_1 tip-sample distance, where P and AP denote parallel and antiparallel tip magnetization directions, respectively, compared to a predefined direction. From these two measured spectra, the magnetic contribution to the differential conductance can be calculated as

$$\frac{dI_{MAGN}^A}{dV}(z_1,V)=\frac{1}{2}\left[\frac{dI_P^A}{dV}(z_1,V)-\frac{dI_{AP}^A}{dV}(z_1,V)\right]. \quad (1)$$

Using this quantity, the magnetic current can be determined at arbitrary V bias voltages via integration:

$$I_{MAGN}^A(z_1,V)=\int_0^V d\tilde{V}\frac{dI_{MAGN}^A}{d\tilde{V}}(z_1,\tilde{V}). \quad (2)$$

---

*Electronic address: palotas@phy.bme.hu

Here, we assumed zero temperature. For a given surface-tip combination, by varying the upper integral limit V, we can determine the bias voltage, where the magnetic current is zero. This corresponds to a magnetic contrast reversal on the constant current SP-STM image, as will be demonstrated later. This bias position can be found using magnetic tips having arbitrary magnetization direction, however, the contrast can further be enhanced by setting the tip magnetization direction properly as discussed in Ref. [13]. Thus, from P and AP single point spectra measured at tip position (A, z_1), the bias voltage(s) can be determined, where a magnetic contrast reversal occurs.

Similarly to the magnetic current, the topographic current can be calculated from the same single point P and AP spectra as

$$\begin{aligned} \frac{dI^A_{TOPO}}{dV}(z_1,V) &= \frac{1}{2}\left[\frac{dI^A_P}{dV}(z_1,V)+\frac{dI^A_{AP}}{dV}(z_1,V)\right], \quad (3)\\ I^A_{TOPO}(z_1,V) &= \int_0^V d\tilde{V}\frac{dI^A_{TOPO}}{d\tilde{V}}(z_1,\tilde{V}), \quad (4)\end{aligned}$$

and the total current with P tip alignment is

$$I^A(z_1,V) = I^A_{TOPO}(z_1,V) + I^A_{MAGN}(z_1,V). \quad (5)$$

The same procedure can be repeated above atom B, i.e. P and AP single point spectra have to be measured, and the corresponding currents can be calculated similarly to atom A, e.g. $I^B(z_1,V)$ denotes the total current with P tip alignment at the tip-sample distance z_1 and bias voltage V.

In an SP-STM image of a complex magnetic surface the magnetic modulation is superimposed on top of the topographic image. Generalizing the relation between constant current and constant height STM images reported in Ref. [14] to SP-STM images, we can define the contrast between atoms A and B on the surface at the tip-sample distance z_1 and bias voltage V as

$$\begin{aligned}\Delta z_{AB}(z_1,V) &= -\frac{\Delta I^{AB}(z_1,V)}{\partial I_{TOPO}/\partial z(z_1,V)}\\ &= \frac{I^A(z_1,V)-I^B(z_1,V)}{2\kappa_0(V)I_{TOPO}(z_1,V)}, \quad (6)\end{aligned}$$

where the average tip-sample distance has been generalized to the topographic image, i.e. the constant current contour of the nonmagnetic part of the tunneling current, I_{TOPO}. We also took advantage of the exponentially decaying character of the tunneling current, $I_{TOPO}(z,V) = I_0(V)e^{-2\kappa_0(V)z}$. The contrast in Eq.(6) corresponds to the apparent height difference of atom A and B on a proper constant current contour, and can be decomposed to topographic and magnetic parts,

$$\begin{aligned}\Delta z_{AB}(z_1,V) &= \Delta z^{AB}_{TOPO}(z_1,V) + \Delta z^{AB}_{MAGN}(z_1,V)\\ &= \frac{I^A_{TOPO}(z_1,V)-I^B_{TOPO}(z_1,V)}{2\kappa_0(V)I_{TOPO}(z_1,V)}\\ &+ \frac{I^A_{MAGN}(z_1,V)-I^B_{MAGN}(z_1,V)}{2\kappa_0(V)I_{TOPO}(z_1,V)}. \quad (7)\end{aligned}$$

If the topographic contrast Δz^{AB}_{TOPO} is zero, then the total contrast in Eq.(6) corresponds to the magnetic contrast. This happens, e.g., on surfaces consisting of chemically equivalent but magnetically inequivalent atoms. In this case $I_{TOPO} = I^A_{TOPO} = I^B_{TOPO}$. In order to be able to calculate the so far unknown decay $\kappa_0(V)$, a third pair of single point P and AP spectra is needed at a different tip-sample distance z_2, e.g., above atom A. Since I^A_{TOPO} can be calculated from the spectra according to Eq.(4) at both tip-sample distances, and the tip displacement $z_2 - z_1$ can be measured in experiments, the decay can be determined as

$$\kappa_0(V) = \frac{\ln I^A_{TOPO}(z_1,V) - \ln I^A_{TOPO}(z_2,V)}{2(z_2-z_1)}. \quad (8)$$

Thus, by measuring P and AP tunneling spectra in each of the three well-defined tip positions above the surface: (A, z_1), (A, z_2), and (B, z_1), the bias dependent magnetic contrast between atom A and B at the tip-sample distance z_1, $\Delta z_{AB}(z_1,V)$, can be predicted following Eq.(6). From this function the bias position can be identified, where the maximal magnetic contrast can be achieved. Since the magnetic contrast is assumed to be exponentially decaying with respect to the tip-sample distance similarly to the corrugation amplitude of nonmagnetic STM images, the identified bias position of the maximal magnetic contrast should not change by recording SP-STM images at different constant current conditions, i.e. at different tip-sample distances.

By additionally recording P and AP tunneling spectra at the tip position (B, z_2), $\Delta z_{AB}(z_2,V)$ can also be calculated. Thus, measured spectra at four well-defined tip positions above the surface: (A, z_1), (A, z_2), (B, z_1), and (B, z_2) are, in principle, sufficient for determining the bias dependent magnetic contrast between atom A and B at an *arbitrary* tip-sample distance z in the tunneling regime:

$$\Delta z_{AB}(z,V) = [\Delta z_{AB}(z_1,V)]^{\frac{z_2-z}{z_2-z_1}}[\Delta z_{AB}(z_2,V)]^{\frac{z-z_1}{z_2-z_1}}. \quad (9)$$

Note that since the absolute tip-sample distances are unknown in experiments, the magnetic contrast can be determined at distance z relative to z_1 and z_2 only.

In order to demonstrate the applicability of the proposed procedure for estimating the bias dependent magnetic contrast from single point tunneling spectroscopy data, we perform simulations on a sample surface with noncollinear magnetic order. One monolayer (ML) Cr on Ag(111) is a prototype of frustrated hexagonal antiferromagnets [14]. Due to the geometrical frustration of the antiferromagnetic exchange interactions between the Cr spin moments, its magnetic ground state is a noncollinear 120° Néel state [15]. Taking the spin-orbit coupling into account, two Néel states with opposite chiralities can form, and one of them is energetically favored [9].

We performed fully noncollinear electronic structure calculations on the Cr/Ag(111) system, based on the density functional theory (DFT) within the generalized gradient approximation (GGA) and using the projector augmented wave (PAW) method, implemented in the Vienna ab initio simulation package (VASP) [16–20]. The computational details are reported elsewhere [9]. We used two tip models: one is an electronically flat, maximally spin-polarized ($P_T = +1$) ideal magnetic tip, and the second is a blunt Ni tip, i.e. a Ni adatom placed above the hollow position of a Ni(110) surface. More details on the chosen tip models can be found in Ref. [13].

Taking the calculated electronic structures, the differential conductances can be obtained following Ref. [21]. On the other hand, the magnetic current can directly be determined from the sample and the tip electronic structures at the tip apex position $\underline{R}_{TIP}$ above the sample surface using the atom superposition method [9, 14, 22, 23] based on the spin-polarized Tersoff-Hamann model [15, 24, 25], assuming elastic tunneling:

$$\begin{aligned} &I_{MAGN}(\underline{R}_{TIP},V) \\ &\propto \int_0^V dU \sum_\alpha \underline{m}_S^\alpha(E_F^S+eU)\,\underline{m}_T(E_F^T-eV+eU) \\ &\times\; e^{-\frac{2}{\hbar}\sqrt{2m\left(\frac{\phi_S+\phi_T+eV}{2}-eU\right)}|\underline{R}_{TIP}-\underline{R}_\alpha|}. \end{aligned} \qquad (10)$$

Here, the sum over α includes a sufficient number of surface atoms [13] with position $\underline{R}_\alpha$ and projected magnetic density of states (magnetic DOS), $\underline{m}_S^\alpha$. Similarly, $\underline{m}_T$ denotes the magnetic density of states projected onto the tip apex atom. E_F^S and E_F^T are the Fermi energies of the surface and the tip, respectively. Moreover, the exponential expression is the tunneling transmission assuming spherical decay of the electron wave functions and an effective rectangular tunnel barrier, where ϕ_S and ϕ_T are the surface and tip electron work functions, respectively. The shape of the electron orbitals involved in the tunneling [26] are neglected (independent orbital approximation [14]).

Figure 1 shows the simulated magnetic current, $I_{MAGN}(V)$, according to Eq.(10) $z = 3.5$ Å above each Cr atom (Cr1, Cr2, Cr3) in the $(\sqrt{3}\times\sqrt{3})$ magnetic unit cell shown in the left part of Figure 3, measured with the two considered tip models. For the negative bias range, the integral limits are reversed in order to obtain positive total current values, and the magnetic current has been calculated accordingly. The tip magnetization direction is fixed parallel to the Cr1 magnetic moment. Due to the frustrated magnetic structure, the Cr2 and Cr3 magnetic moments have an angle of 120° with respect to the tip magnetization direction. Following this, the magnetic currents measured above the Cr2 and Cr3 surface atoms are equal and their values are $\cos(120°) = -0.5$ times the magnetic current above Cr1. Moreover, it is clearly demonstrated in Figure 1 that the magnetic properties of the tip affect the magnetic current considerably.

The magnetic contrast is reversed at $I_{MAGN}(V) = 0$. In order to find out the corresponding bias positions for the two considered tips, we have to zoom in the region [0 V, 1 V]. The indicated rectangular area is shown in the inset of Figure 1. It is clearly seen that the sign change of $I_{MAGN}(V)$ occurs at 0.94 V and 0.74 V for the ideal and the Ni tip, respectively. Although the reversal is, in principle, due to the surface electronic structure [8, 9], the tip plays a crucial role as well, since its electronic structure modifies the bias position of the reversal. Note that the determination of the above bias positions does not depend on whether the tip is placed above Cr1, Cr2, or Cr3 atoms. Moreover, we find that the bias voltage of the contrast reversals is stable within ±0.01 V placing the tip above other surface positions.

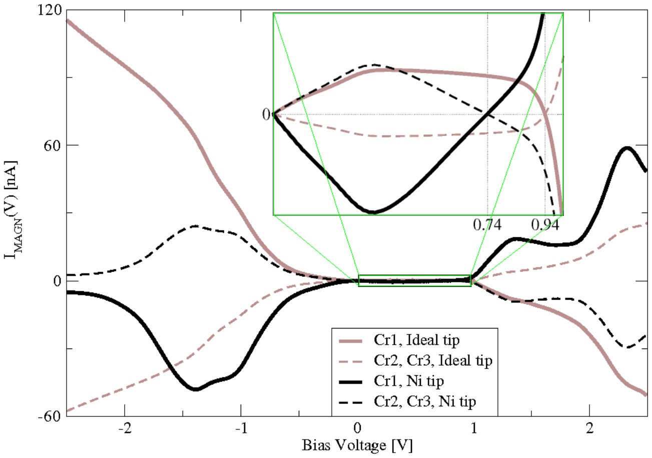

FIG. 1: (Color online) Simulated magnetic current, $I_{MAGN}(V)$, according to Eq.(10) $z = 3.5$ Å above each Cr atom (Cr1, Cr2, Cr3) in the $(\sqrt{3}\times\sqrt{3})$ magnetic unit cell (see left part of Figure 3), measured with an ideal electronically flat maximally spin-polarized tip (gray), or a model Ni tip (black). The tip magnetization direction is fixed parallel to the Cr1 magnetic moment in Figure 3. The inset shows the region between 0 V and 1 V zoomed in. The sign change of $I_{MAGN}(V)$ occurs at 0.94 V and 0.74 V for the ideal and the Ni tip, respectively. These correspond to magnetic contrast reversals.

In order to estimate the bias dependent magnetic contrast, Eq.(6) has to be employed. The topographic current I_{TOPO} can be calculated similarly to Eq.(10) by replacing the magnetic DOS by the corresponding charge DOS of the sample and the tip [9]. The decay of $I_{TOPO}(z,V)$ can be calculated using Eq.(8). In the simulations we determined $\kappa_0(V)$ from $I_{TOPO}(z,V)$ by linear regression taking 150 z values in the range [0.01 Å, 7.95 Å] at each chosen bias voltage with 0.01 V steps in the [-2.5 V, 2.5 V] interval. Figure 2 shows the bias dependent magnetic contrast between Cr1 and Cr3 atoms at two different tip-sample distances using both tip models. The sign of the curves corresponds to the ones denoted by solid line in Figure 1, and the contrast reversal is obtained at $\Delta z_{Cr1-Cr3}(z,V) = 0$. However, due to the denominator of Eq.(6), we obtain qualitatively different curves compared to Figure 1. From the calculated functions, bias voltages can be identified in both the negative

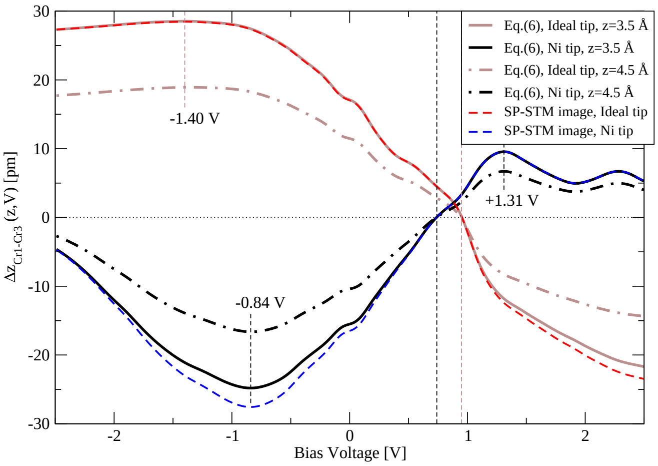

FIG. 2: (Color online) The bias dependent magnetic contrast between Cr1 and Cr3 atoms $\Delta z_{Cr1-Cr3}(z,V)$ at two different tip-sample distances, $z = 3.5$ Å (solid lines) and $z = 4.5$ Å (dash-dotted lines) calculated using Eq.(6) measured with the ideal magnetic tip (gray) and the Ni tip (black). The local absolute maxima of the magnetic contrasts and their bias values are explicitly shown in both the negative and the positive bias ranges. Vertical dashed lines denote the contrast reversals, see also Figure 1. For comparison, color dashed lines show the apparent height difference between Cr1 and Cr3 atoms calculated from constant current SP-STM images, see text for details.

and positive bias ranges, where a local absolute maximum magnetic contrast can be achieved. As can be seen, these highly depend on the properties of the magnetic tip. In the studied bias interval local absolute maximum contrasts are expected at -1.40 V and 2.50 V for the measurement with the ideal tip, whereas these bias values are considerably modified to -0.84 V and 1.31 V by using the Ni tip. The maximum absolute contrasts are obtained at the corresponding negative bias values for both tips. Moreover, as can be seen, the change of the tip-sample distance does not modify the bias positions of the absolute contrast maxima. We tested it for other distances as well, and the bias positions were found within ±0.02 V.

For comparison, color dashed lines in Figure 2 show the apparent height difference between Cr1 and Cr3 atoms calculated from constant current SP-STM images. The current contour was chosen in such a way that the apparent height of the Cr1 atom is 3.5 Å at all considered bias voltages. The agreement with the estimated magnetic contrast using Eq.(6) is remarkable, particularly for $\Delta z_{Cr1-Cr3} > 0$. There are some quantitative deviations if $\Delta z_{Cr1-Cr3}$ is negative, but the overall qualitative bias dependence is well reproduced by Eq.(6).

In order to better visualize the bias dependent contrast, we simulated constant current SP-STM images. Figure 3 shows such images measured with the ideal magnetic tip (top row) and the Ni tip (bottom row) at 0 V, at the bias voltages corresponding to the contrast reversal (0.94 V and 0.74 V, respectively), and at the voltages corresponding to the local absolute maxima of the magnetic contrast in both the negative and positive ranges. The surface geometry is shown in the left part of the figure, together with the scanning area (black-framed rectangle), and the magnetic unit cell (yellow (light gray) framed rhombus). The tip magnetization direction is parallel to the Cr1 magnetic moment. For the zero bias images a temperature of 4.2 K has been considered following Ref. [9], since there is no current at 0 K.

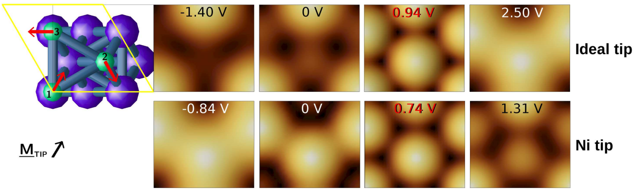

FIG. 3: (Color online) Simulated SP-STM images depending on the bias voltage and the considered tip: ideal magnetic tip (top row), Ni tip (bottom row). The magnetic moment of the tip apex atom is parallel to Cr1, and indicated by a vector ($\underline{M}_{TIP}$). The surface geometry of 1 ML Cr on Ag(111) and its ground state magnetic structure are explicitly shown. The Cr and Ag atoms are denoted by spheres colored by green (medium gray) and purple (dark gray), respectively, while the magnetic moments of individual Cr atoms are indicated by (red) arrows. The $(\sqrt{3} \times \sqrt{3})$ magnetic unit cell is drawn by yellow (light gray) color, and the scanning area is shown by the black-framed rectangle.

We find a similar type of magnetic contrast at 0 V and at the negative bias voltages for both tips, respectively, i.e., for $V < 0$, $\Delta z_{Cr1-Cr3} > 0$ (Cr1 appears higher than Cr2 and Cr3) for the ideal tip, and $\Delta z_{Cr1-Cr3} < 0$ (Cr1 appears lower than Cr2 and Cr3) for the Ni tip, similarly as reported in Figure 2. At the corresponding reversal voltages, 0.94 V (ideal tip) and 0.74 V (Ni tip), all Cr atoms appear to be of equal height on the SP-STM image. Here, the magnetic contrast is lost as $I_{MAGN} = 0$. This corresponds to a qualitatively similar image of performing the STM measurement with a nonmagnetic tip [9]. Thus, the magnetic current calculated at a single point above the surface was indeed able to find the correct bias position of the magnetic contrast reversal. At biases above the reversal voltage, the magnetic contrast is inverted. We illustrate this for the image calculated at 2.50 V for the ideal tip, and at 1.31 V for the Ni tip.

In conclusion, we proposed a procedure for determining the bias dependent magnetic contrast from single point differential conductance tunneling spectra measured with oppositely magnetized tips. By performing simulations based on first principles electronic structure calculations, we demonstrated that the obtained bias dependent contrast corresponds well to the apparent height difference calculated from constant current SP-STM images. Our theoretical prediction should inspire experimentalists to considerably reduce measurement efforts for determining the bias dependent magnetic contrast on magnetic surfaces.

The author thanks László Szunyogh for useful comments on the manuscript. Financial support of the Magyary Foundation, EEA and Norway Grants, the Hungarian Scientific Research Fund (OTKA PD83353, K77771), the Bolyai Research Grant of the Hungarian Academy of Sciences, and the New Széchenyi Plan of Hungary (Project ID: TÁMOP-4.2.2.B-10/1–2010-0009) is gratefully acknowledged. Furthermore, partial usage of the computing facilities of the Wigner Research Center for Physics is kindly acknowledged.

---

[1] E. M. L. Plumer, J. van Ek, and D. Weller, *The Physics of Ultra-High Density Magnetic Recording, Springer Series in Surface Science Vol. 41* (Springer, Berlin, Germany, 2001).
[2] N. Weiss, T. Cren, M. Epple, S. Rusponi, G. Baudot, S. Rohart, A. Tejeda, V. Repain, S. Rousset, P. Ohresser, F. Scheurer, P. Bencok, and H. Brune, Phys. Rev. Lett. **95**, 157204 (2005).
[3] D. Serrate, P. Ferriani, Y. Yoshida, S.-W. Hla, M. Menzel, K. von Bergmann, S. Heinze, A. Kubetzka, and R. Wiesendanger, Nature Nanotechnology **5**, 350 (2010).
[4] M. Bode, Rep. Prog. Phys. **66**, 523 (2003).
[5] R. Wiesendanger, Rev. Mod. Phys. **81**, 1495 (2009).
[6] W. Wulfhekel and C. L. Gao, J. Phys. Condens. Matter **22**, 084021 (2010).
[7] S. Heinze, K. von Bergmann, M. Menzel, J. Brede, A. Kubetzka, R. Wiesendanger, G. Bihlmayer, and S. Blügel, Nature Physics **7**, 713 (2011).
[8] R. Yang, H. Yang, A. R. Smith, A. Dick, and J. Neugebauer, Phys. Rev. B **74**, 115409 (2006).
[9] K. Palotás, W. A. Hofer, and L. Szunyogh, Phys. Rev. B **84**, 174428 (2011).
[10] M. Waśniowska, S. Schröder, P. Ferriani, and S. Heinze, Phys. Rev. B **82**, 012402 (2010).
[11] W. A. Hofer, K. Palotás, S. Rusponi, T. Cren, and H. Brune, Phys. Rev. Lett. **100**, 026806 (2008).
[12] A. A. Khajetoorians, J. Wiebe, B. Chilian, and R. Wiesendanger, Science **332**, 1062 (2011).
[13] K. Palotás, W. A. Hofer, and L. Szunyogh, Phys. Rev. B **83**, 214410 (2011).
[14] S. Heinze, Appl. Phys. A **85**, 407 (2006).
[15] D. Wortmann, S. Heinze, P. Kurz, G. Bihlmayer, and S. Blügel, Phys. Rev. Lett. **86**, 4132 (2001).
[16] G. Kresse and J. Furthmüller, Comput. Mater. Sci. **6**, 15 (1996).
[17] G. Kresse and J. Furthmüller, Phys. Rev. B **54**, 11169 (1996).
[18] G. Kresse and D. Joubert, Phys. Rev. B **59**, 1758 (1999).
[19] D. Hobbs, G. Kresse, and J. Hafner, Phys. Rev. B **62**, 11556 (2000).
[20] D. Hobbs and J. Hafner, J. Phys. Condens. Matter **12**, 7025 (2000).
[21] K. Palotás, W. A. Hofer, and L. Szunyogh, Phys. Rev. B **85**, 205427 (2012).
[22] H. Yang, A. R. Smith, M. Prikhodko, and W. R. L. Lambrecht, Phys. Rev. Lett. **89**, 226101 (2002).
[23] A. R. Smith, R. Yang, H. Yang, W. R. L. Lambrecht, A. Dick, and J. Neugebauer, Surf. Sci. **561**, 154 (2004).
[24] J. Tersoff and D. R. Hamann, Phys. Rev. Lett. **50**, 1998 (1983).
[25] J. Tersoff and D. R. Hamann, Phys. Rev. B **31**, 805 (1985).
[26] K. Palotás, G. Mándi, and L. Szunyogh, arXiv:1206.6628 , (2012).